Impact of Identification Method on the Inferred Characteristics and Variability of Australian East Coast Lows

ACACIA S. PEPLER AND ALEJANDRO DI LUCA

Centre for Excellence for Climate System Science and Climate Change Research Centre, University of New South Wales, Sydney, Australia

FEI JI

New South Wales Office of Environment and Heritage, Sydney, Australia

LISA V. ALEXANDER, JASON P. EVANS, AND STEVEN C. SHERWOOD

Centre for Excellence for Climate System Science and Climate Change Research Centre, University of New South Wales, Sydney, Australia

ABSTRACT

The Australian east coast low (ECL) is both a major cause of damaging severe weather and an important contributor to rainfall and dam inflow along the east coast, and is of interest to a wide range of groups including catchment managers and emergency services. For this reason, several studies in recent years have developed and interrogated databases of east coast lows using a variety of automated cyclone detection methods and identification criteria. This paper retunes each method so that all yield a similar event frequency within the ECL region, to enable a detailed intercomparison of the similarities, differences, and relative advantages of each method. All methods are shown to have substantial skill at identifying ECL events leading to major impacts or explosive development, but the choice of method significantly affects both the seasonal and interannual variation of detected ECL numbers. This must be taken into consideration in studies on trends or variability in ECLs, with a subcategorization of ECL events by synoptic situation of key importance.

1. Introduction

On the east coast of Australia, east coast lows (ECLs) can cause heavy rain, strong winds, and high seas (e.g., Abbs et al. 2006; Callaghan and Helman 2008; Speer et al. 2009; Dowdy et al. 2014), resulting in major flooding, loss of life, and interruptions to shipping. Hopkins and Holland (1997) identified that 7% of all major natural disasters in Australia between 1967 and 1991 were a consequence of ECLs, while an ECL in June 2007 caused close to $1.5 billion [Australian dollars (AUD)] in damage, including the beaching of the bulk carrier "Pasha Bulker" (Mills et al. 2010; Chambers et al. 2014). This is the seventh-largest disaster loss in Australia since records began in 1967, when normalized to account for inflation.[1] In addition, ECLs are a major contributor to annual rainfall totals and catchment inflows along the coast, with important implications for rainfall variability and water security (Pepler and Rakich 2010; Pepler et al. 2014). For these reasons, ECLs are of major interest to sectors ranging from emergency managers to catchment authorities.

An ECL can be loosely described as any surface low pressure system that forms or intensifies in a maritime environment near the east coast (Speer et al. 2009; see solid line in Fig. 1). The term ECL can, thus, include systems ranging from deep extratropical cyclones with attached frontal systems, to mesoscale lows developing

---

Corresponding author address: Acacia S. Pepler, Climate Change Research Centre, High St., University of New South Wales, Sydney, NSW 2052, Australia.
E-mail: a.pepler@student.unsw.edu.au

[1] Insurance Council of Australia Limited. Major disasters since June 1967 (accessed May 2014; http://www.insurancecouncil.com.au/industry-statistics-data/disaster-statistics/historical-disaster-statistics).
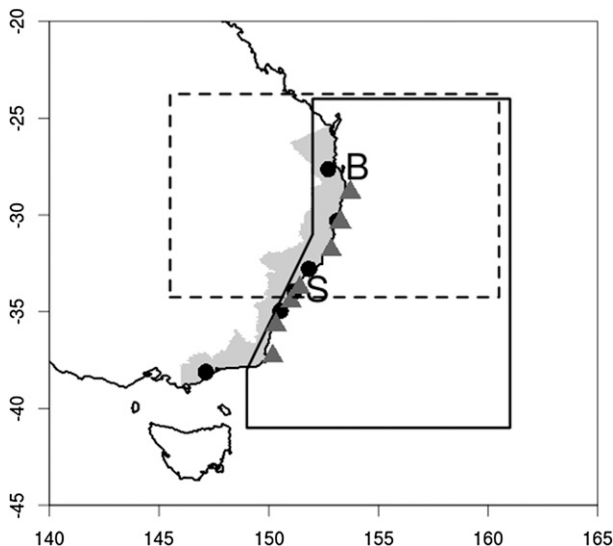
FIG. 1. Southeastern Australia, with key features marked. The solid black lines indicate the domain for identifying ECLs in the surface pressure, while the dashed line indicates the corresponding region for detecting geostrophic vorticity maxima at 500 hPa (note the westward shift relative to the ECL domain). The shaded gray region indicates the area for detection of east coast cluster rain events, while the black circles and gray triangles indicate the wind and wave data, respectively. The "S" and "B" indicate major population centers: Sydney and Brisbane, respectively.

in a coastal trough, to transitioning tropical cyclones. As the ECL region extends to 24°S, northern areas can also be impacted by fully fledged tropical cyclones, with a category 3 cyclone in the Brisbane region causing major damage, flooding, and numerous deaths in February 1954 (Callaghan and Helman 2008; Speer et al. 2009).

Because of the diverse nature of low pressure systems impacting the east coast, there is considerable inconsistency in the identification of ECLs between studies. Historical studies such as Hopkins and Holland (1997), Qi et al. (2006), and Callaghan and Helman (2008) focused on a subset of ECLs identified by the presence of severe impacts in terms of wind, rain, and other criteria, with the most systematic (Hopkins and Holland 1997) identifying an average of 2.5 such events per year between 1958 and 1992. In more recent years, a more comprehensive ECL database was developed by Speer et al. (2009), which was referred to as the maritime low database (MLD). This database includes all surface lows in the region indicated in Fig. 1 between 1970 and 2006, as identified through manual inspection of the 0000 UTC synoptic charts. This database averages 22 ECLs per year, many of which have no identified weather impacts on the Australian coast.

The issue of identifying ECLs persists to the present day. Over recent decades, there has been significant progress in the use of objective low tracking algorithms

to supplement or replace subjective and labor-intensive subjective databases such as the MLD (e.g., Murray and Simmonds 1991; König et al. 1993; Sinclair 1994; Hoskins and Hodges 2005; Wernli and Schwierz 2006). Several of these studies have analyzed broader patterns of extratropical cyclone activity across the Southern Hemisphere, and an international study is currently under way to compare 15 low tracking schemes across the globe (Neu et al. 2013). This found relatively high consistency between identification methods for strong lows, but large differences in absolute numbers of storms, particularly when considering small, short-lived and slowly moving cyclones.

These broadscale studies offer a more robust comparison than is possible for this paper, comparing large numbers of tracking schemes across several reanalysis datasets. However, because of their global scale and large variations in cyclone frequency they offer limited insight into the finer details of tracking scheme performance in small regions such as the east coast of Australia. Furthermore, use of a manual database for comparisons in this study offers the ability to tease out the skill of each scheme for ECLs that develop in different synoptic systems and those associated with severe weather impacts.

In the past three years, two studies have instead sought to apply similar low tracking algorithms specifically to the Australian ECL (Browning and Goodwin 2013; Pepler and Coutts-Smith 2013), with a third study (Dowdy et al. 2011) attempting to identify ECL-favorable conditions in the upper-level circulation. Each study employed a different low identification method and optimized it to the Australian region, using the MLD described above as a baseline for comparison. Therefore, there is a need to understand the extent to which the results using these different ECL detection methods differ, to give guidance for future users in choosing the ECL identification method best suited to their needs.

In this paper, we first describe the Speer et al. (2009) MLD and the four automated ECL identification methods used in this study, including any modifications from the initial paper. The ECLs identified using each detection method are compared in terms of their seasonality, spatial distribution, and other characteristics, with the proviso that some data are unavailable for the Dowdy et al. (2011) method. We then compare the extent to which the different automated methods detect the same ECL events, with particular focus on the detection of ECLs associated with severe weather impacts or rapid (explosive) development. For this purpose, the MLD can be used as a benchmark, with the expectation that all major or impactful events are included, although it cannot be considered as "truth." Finally, we present
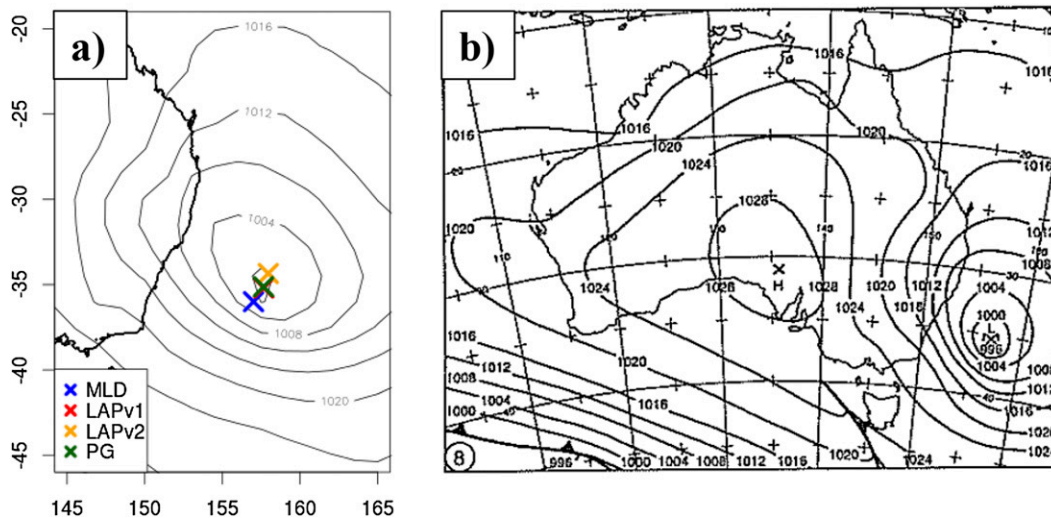
FIG. 2. (a) The ERA-Interim MSLP field for a deep ECL at 0000 UTC 8 Aug 1998, with ECL locations for four approaches marked. The corresponding 2-day mean maximum geostrophic vorticity at 500 hPa for this time was 7.1 × $10^{-5}\,\text{s}^{-1}$. (b) The corresponding Bureau of Meteorology synoptic chart obtained from the *Monthly Weather Review-Australia*; note the similarity of central pressure and contour separation between the two analyses.

a summary of the advantages and disadvantages of each method, to help future users identify the approach of greatest use.

2. ECL databases

a. The maritime low database

The MLD is a comprehensive, manual database of ECL events that was developed within the Australian Bureau of Meteorology, and is described by Speer et al. (2009). This database was built on the archived mean sea level pressure charts that were prepared by the forecasters at the National Meteorological and Oceanographic Centre, of which the 0000 UTC surface chart was readily accessible as part of the bureau's *Monthly Weather Review-Australia* series (http://www.bom.gov. au/climate/mwr; an example is shown in Fig. 2b). A skilled observer then identified all cases where a surface low was indicated by either a closed contour or a low center ("L" or "X") in the region indicated by the solid line in Fig. 1, with only the deepest low retained in cases with multiple centers. For each instance the database includes the latitude, longitude, and central pressure of the low, with lows on consecutive days combined into ECL events based on the judgment of the analyst. While pressure data was the main information used, records of impacts were also taken into account by the analyst, with satellite data used to aid identification in some instances in later years. This approach has high costs in terms of human resources, with the database restricted to the period 1970–2006.

The MLD also includes additional information on the synoptic situation of the ECL. While Speer et al. (2009) identified six different ECL types, we employ their more general three-category system of lows that develop in easterly (E) wind regimes (easterly trough and inland trough lows) versus lows that develop from the mid-latitude westerlies (W; decaying fronts, waves on a front, and lows in the westerlies), in addition to ex-tropical cyclones. Because of the requirement of a low center, the database excludes precyclonic frontal waves [i.e., Hewson (2009) stages 0–2]. While these can develop into substantial cyclonic storms in the North Atlantic, the frequency and importance of such events along the east coast of Australia is yet to be quantified, so the influence on this study is uncertain.

Speer et al. (2009) defined an ECL as a "bomb" where a 10-hPa or larger decrease in pressure was observed over 24 h. This threshold is either applied to the difference in central pressure at two consecutive (24 h) time steps, or the difference between the central pressure at the first instance where a low is defined and the average pressure in the previous chart, to accommodate cases where the strength of the first identifiable time for an event indicates rapid development occurred in the preceding 24 h. This database identified 2.5 explosive ECLs per year from visual analysis, many of which were based on the "instantaneous" appearance of a strong low between two consecutive 24-h charts.

The advantage of this approach is that it uses human pattern recognition to identify ECL events, with the added capability to classify ECL events based on the

broader synoptic situation. While the MLD cannot be taken as truth, its subjective nature means it will include most ECLs with significant impacts during the period of overlap, 1980–2006. For this reason, the MLD makes a useful ground truth for testing the automated schemes and can be treated as a baseline for comparisons. However, the subjective nature of ECL identification may result in inconsistent identification of lows, particularly borderline or weak events and those near the boundary of the ECL region. The approach also suffers from low temporal resolution, and is known to miss events where development or movement is sufficiently rapid that the event is present in the ECL domain for less than 24 h, and, therefore, outside the domain for both 0000 UTC charts (Pepler and Coutts-Smith 2013).

b. Automated low detection methods

The ECLs identified in the MLD will be compared to those derived using four different automated low detection methods, all of which have been applied to the Australian ECL in recent years (Dowdy et al. 2011; Browning and Goodwin 2013; Pepler and Coutts-Smith 2013). Such methods can be applied to any set of gridded pressure observations, with the 1.5° Interim European Centre for Medium-Range Weather Forecasts (ECMWF) Re-Analysis (ERA-Interim; Dee et al. 2011) chosen for this study based on its use for the original versions of two of the three recent studies (Browning and Goodwin 2013; Dowdy et al. 2013b). From this reanalysis, surface pressure and upper-level geostrophic height data were retrieved at 6-hourly intervals between 1980 and 2009, with one example field shown in Fig. 2a.

The choice of reanalysis dataset has little influence on the detection of ECLs at low spatial resolutions (e.g., Neu et al. 2013). We tested the sensitivity of results to reanalysis choice by also applying each tracking scheme to the 2.5° National Centers for Environmental Prediction–National Center for Atmospheric Research (NCEP–NCAR) reanalysis (Kalnay et al. 1996), which resulted in similar patterns of seasonality, interannual variability, and event detection for each method (not shown), giving some confidence in the robustness of results. However, it is important to note that lower-resolution reanalyses can fail to detect the true intensity of lows, particularly those at small spatial scales (e.g., Uotila et al. 2009), and do not incorporate skilled local knowledge for subgrid-scale lows such as is available for the MLD. While a higher spatial resolution of ERA-Interim is now available, this was not used because of the large variability in low detection for the same method across different reanalyses at high spatial resolutions (e.g., Di Luca et al. 2014, manuscript submitted to

J. Climate), which would add additional uncertainty to results.

1) THE LAPLACIAN METHOD (LAP)

The cyclone identification and tracking scheme described in Murray and Simmonds (1991) is one of the more widely used low identification methods in the literature (e.g., Lim and Simmonds 2002; Pezza and Ambrizzi 2003; Pinto et al. 2005; Allen et al. 2010; Kouroutzoglou et al. 2011; Grieger et al. 2014), and has recently been applied to the Australian ECL in Pepler and Coutts-Smith (2013). This approach first identifies a maximum in the Laplacian of the pressure, before employing an iterative technique to identify a corresponding pressure minimum from a spline-fitted pressure field. This surface low can be either a low with closed contours, or an "open" system with a strong pressure inflexion, with the "center" of open systems given as the point of minimum pressure gradient. Open systems form less than 5% of identified lows, but are retained to avoid unnecessary splitting of an ECL event that may temporarily lose closed circulation. For each surface low a future position is predicted based on a combination of climatological and previous movement, with the cyclone track determined based on a weighted least squares difference between the predicted and observed position and intensity (described in more detail in Murray and Simmonds 1991).

The Laplacian of MSLP is proportional to the geostrophic vorticity, with the average of the Laplacian within a specified radius of the low center (referred to as the "curvature") an indicator of the intensity of the low; for this reason, in this paper this tracking scheme will be referred to as the Laplacian method (LAP).

Two versions of this scheme are applied in this paper. One corresponds to a relatively old version of the scheme that is maintained by the Bureau of Meteorology (hereafter LAPv1; Jones and Simmonds 1993), which was used in Pepler and Coutts-Smith (2013) when determining the location and duration criteria to distinguish an ECL. The other is the current version of the scheme used at the University of Melbourne (hereafter LAPv2; Simmonds et al. 1999; Lim and Simmonds 2007) that includes several advances and a number of additional input and output parameters compared with the earlier version of the LAP method.

To the extent to which it is possible, the same low identification and tracking parameters have been employed for both versions of this scheme; however, the newer version (LAPv2) has a number of improvements over the older version. These include changes to the calculations of predicted low movement ("steering") and the inclusion of a weak/strong criterion in the

probability matching algorithm, as well as an increase in the number of tunable parameters. The new version also includes additional data smoothing and topographic filtering, of particular value at high spatial resolutions (e.g., Uotila et al. 2009, 2011), which is expected to influence the detection of lows near the coastline. For the purposes of this paper, a smoothing radius of 2° was used, which was found to give the best results for 1.5°–2.5° grids, with all other parameters for which a LAPv1 equivalent is unknown left at the default values.

The intensity of a cyclone detected by this scheme is given by the average of the Laplacian over a defined radius from the center of the low. This intensity measure is sensitive to the choice of radius, with higher curvatures when the average is calculated closer to the center of the low. For this study we use an averaging radius of 2° for both versions of this approach, which is consistent with the use of this tracking algorithm on a variety of 2.5° reanalyses (Simmonds et al. 2008). Note that this is a substantially smaller radius than used with LAPv1 in Pepler and Coutts-Smith (2013), and may improve the detection of smaller lows.

While these two methods are based on the same approach, it is expected that there may still be significant differences, with two versions of this scheme showing surprisingly large differences in Neu et al. (2013). Note also that the newer (LAPv2) approach also first regrids the ERA-Interim pressure field to a polar stereographic grid, to improve its use at polar latitudes, with the projection chosen to give a spatial resolution of 1.5° at 30°S; this is not expected to cause major differences at these latitudes, but has not been tested to our knowledge.

2) THE PRESSURE GRADIENT METHOD (PG)

Browning and Goodwin (2013) identified east coast lows based on the presence of a closed low in the surface pressure, in a similar approach to Alpert et al. (1990), with closed lows identified and tracked using the 1.5° ERA-Interim reanalysis. As the average pressure gradient is used to decide on the existence of a cyclone and to indicate the intensity of the cyclone, this method will be referred to as the pressure gradient (PG) approach.

This paper employs a slightly modified pressure gradient approach, described in Di Luca et al. (2014, manuscript submitted to *J. Climate*). Prior to the application of the algorithm, the 6-hourly ERA-Interim MSLP fields were regridded into a 10-km regular grid mesh using a bicubic spline interpolation method, in order to account for the likely variation of the pressure field between grid points. As argued by Murray and Simmonds (1991) and Pinto et al. (2005), such interpolation does not add any new information but is believed to be a better approximation of the unknown real field, improving the localization of lows as well as potentially improving measures of cyclone intensity (e.g., Haak and Ulbrich 1996; Pinto et al. 2005).

Closed lows are then identified by searching for both a local minimum in the regridded MSLP field and a mean pressure gradient within 200 km of the local minimum that exceeds a given threshold. In cases where multiple lows are identified within 600 km of each other, only the most intense low is retained. Once cyclones have been detected for all 6-hourly fields, cyclone tracks are constructed by a nearest-neighbor search in the subsequent MSLP field, using a maximum distance of 350 km.

3) THE UPPER-LEVEL GEOSTROPHIC VORTICITY METHOD (ULGV)

Dowdy et al. (2011, 2013c, 2014) presented an alternative method of identifying ECL-favorable conditions that has been optimized for studies using low-resolution global climate models. Rather than seeking to identify an ECL in the pressure field, this approach instead calculates the 500-hPa geostrophic vorticity at each point in the ERA-Interim grid relative to the four surrounding points at each time step, before then calculating the maximum value in the region 23.75°–34.25°S, 145.5°–160.5°E. This region is somewhat different to the area where ECLs are identified in the methods that identify surface lows (see dashed line in Fig. 1), but was found to have the highest detection rates when validated against ECLs in the MLD dataset by Dowdy et al. (2011), so is retained for this study. ECL conditions are then identified where the 48-h running average of the maximum geostrophic vorticity is greater than a specified threshold. This approach will be referred to as the upper-level geostrophic vorticity (ULGV) approach, consistent with the terminology in Dowdy et al. (2011, 2013a).

This approach has been shown to have considerable ability to detect days with significant ECLs, particularly those associated with widespread coastal rain or large waves (Dowdy et al. 2011, 2013a, 2014). However, it is important to note that the presence of an upper-level low does not necessarily indicate a corresponding surface low, particularly as this method identifies longer periods of ECL-favorable conditions. This method consequently does not have location, track, or minimum pressure data available, so will not be used for all comparisons.

3. Data and methods

Each of the low tracking methods has a large number of tunable parameters, which can cause substantial variability in the numbers of ECLs identified. While the

TABLE 1. Annual average and standard deviation of the number of ECL events, as well as the annual average number of days with ECLs observed, and the number of ECL days with associated weather impacts as described in section 2, 1980–2009. Results are for 1980–2006 for the MLD and 1980–2009 for the four automated ECL detection methods.

	MLD	LAPv1	LAPv2	PG	ULGV
Threshold		1	1	0.95	-5.1×10^{-5}
Units		hPa $(°\text{lat})^{-2}$	hPa $(°\text{lat})^{-2}$	hPa $(100\,\text{km})^{-1}$	s^{-1}
Events	22.4	23.4	21.4	22.4	22.4
Σ	4.5	5.9	4.9	6.0	3.3
Days	36.2	35.5	35.6	30.7	75.6
Rain days	15.1	11.4	10.1	9.9	21.3
Wave days	10.4	9.7	9.4	8.1	16.0
Wind days	2.0	3.2	3.3	2.9	4.6

majority of parameters have been set at the values used in their originating studies, we chose to apply thresholds based on the internal criteria of low intensity from each method, in order to restrict analyses to a subset of approximately 22 ECLs per year, approximating the numbers observed in the MLD. This is similar to the approach used for ECLs in Dowdy et al. (2011, 2013a), as well as for front identification schemes in other studies (e.g., Hope et al. 2014), and is expected to give the best possible comparison of the similarities and differences in the characteristics of ECLs identified by each method. In each case, the intensity threshold is applied to the individual lows composing each event, rather than the average or maximum intensity of the ECL event as a whole; this may result in separation of extended ECLs into two events if it exhibits weakening and reintensification. While this approach has been used before, it is important to note that there are several other parameters that could be altered to change the numbers of lows, which would potentially give different results to this study.

The thresholds used for each method are given in Table 1. Note that the thresholds for both LAP methods are substantially stronger than the 0.25 hPa $(°\text{lat})^{-2}$ used in Pepler and Coutts-Smith (2013), which calculated the curvature over a larger radius as well as including more "weak" lows. The threshold for PG is also slightly stronger than the 1 hPa $(1.5°)^{-1}$ in Browning and Goodwin (2013), related to the inclusion of lows with durations below 18 h, while the ULGV threshold is the 85th percentile rather than the 90th (Dowdy et al. 2013a).

A common definition of what constitutes an ECL was also required for the PG and LAP methods, which are able to detect and track individual lows. For each of these an ECL is defined as any low pressure system that persists for at least two consecutive time steps (i.e., more than 6 h) and crosses through the region denoted by the solid line in Fig. 1, with an "ECL event" referring to the entire period for which an individual low is tracked.

While broadscale studies typically require lows to persist for at least 24 h (e.g., Neu et al. 2013), this shorter duration allows improved detection of short-lived embedded lows or broken tracks (Pepler and Coutts-Smith 2013).

These methods are also able to identify lows with explosive development, also known as bombs, which exhibit rapid intensification and can have significant impacts (Sanders and Gyakum 1980; Lim and Simmonds 2002; Allen et al. 2010). While an explosive cyclone is traditionally defined where the 24-h normalized deepening rate (NDR) is greater than 1, because of the short life span of many events we instead use a 6-h normalized deepening rate:

$$\text{NDR} = \frac{\Delta p}{6}\frac{\sin 60}{\sin\theta} \geq 1,$$

where Δp is the pressure change in hPa and θ is the latitude.

At 30°S, a normalized deepening rate of 1 corresponds to a decrease in pressure of 3.5 hPa over 6 h, or 14 hPa over 24 h, slightly stronger than the threshold of 10 hPa over 24 h used in the MLD.

As the ULGV method simply identifies periods of ECL-favorable conditions, it cannot be used to identify and track individual lows or calculate explosive development. For this reason, some analyses will focus on the LAP and PG approaches.

Days are designated as having significant rainfall based on the presence of an eastern seaboard rainfall cluster event as identified by Dowdy et al. (2013a,b) from the Australian Water Availability Project (AWAP) daily gridded rainfall product (Jones et al. 2009); as rain is recorded for the 24 h to 0900 local time (2200 UTC during daylight savings; 2300 UTC, otherwise), these are attributed to ECLs present on the previous day. Note that while the AWAP rainfall data have some issues, particularly in sparsely sampled areas and for high intensity falls, they are expected to perform well on the east coast

where station densities are high, particularly in terms of rainfall with large spatial extent such as is typical for ECLs (King et al. 2013).

A strong wind day is identified when one of six long-record Bureau of Meteorology stations along the east coast records a daily maximum wind gust greater than $90 \, \text{km h}^{-1}$ (Fig. 1), while a strong wave day is identified where the maximum significant wave height is greater than 4 m at any of seven coastal waverider buoys (Manly Hydraulics Laboratory, http://new.mhl.nsw.gov.au/), noting that measurements are unreliable at some buoys prior to 1987. During the period of comparison there are 68.1 days per annum (p.a.), which would be classified as having "severe weather" based on one or more of these three thresholds, approximately 19% of all days.

From this, ECLs are assigned impacts based on a rain, wave or wind day coinciding with any day for which the low is identified. While this approach can incorrectly associate unrelated significant weather to an ECL, manual analysis of ECL cluster rain events (A. Dowdy 2013, personal communication) and strong wind events (Pepler and Coutts-Smith 2013) found that such occasions are rare, and unlikely to impact results.

We can compare the ability of each automated ECL identification method to detect ECL events in the MLD in terms of their hit rates, false alarm rates, and critical success index (CSI), defined as

$$\text{CSI} = \frac{\text{Hits}}{\text{Hits} + \text{Misses} + \text{False Alarms}}.$$

As per Dowdy et al. (2011), both the hit rate and false alarm rate will be calculated using a ± 1-day margin; that is, when comparing to ECL events identified in the MLD, a "hit" occurs when the automated method has an ECL on any day of the event or the two neighboring days, while a false alarm occurs where there are no ECLs in the MLD within ± 1 day of the automated ECL. This avoids penalizing the automated methods due to the low temporal resolution of the MLD. Similar hit rates can be calculated using the 48-h period surrounding the 0000 UTC MLD observation—this causes decreases in hit rates on the order of 2% for all methods, so has little impact on the results of the study. Throughout the paper, correlations are derived using the Pearson's method, while significance is calculated using the Student's t test and assessed at the 5% level.

4. Comparison of ECL statistics

As discussed in section 3, for ease of comparison each automated method has been restricted to a subset of the 22 ECL events per year based on the internal intensity
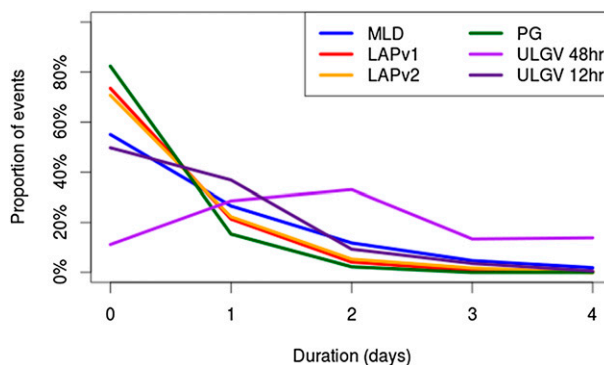

FIG. 3. Distribution of ECL event durations for the MLD and the four automated ECL identification methods (section 2). From 6-hourly MSLP data, a duration of four or fewer time steps represents less than 1 day, 5–8 time steps represents 1 day, etc. Note that the MLD only records ECL information at 0000 UTC daily. A version of the ULGV method with 12-h temporal smoothing is also shown for comparison purposes.

criteria. However, as the lifetime of an individual ECL can vary substantially between events and methods, there is notable variation in the average numbers of ECL days between methods (Table 1). The lifetime of systems within the ECL domain is generally shorter than the MLD (Fig. 3), which is related to the higher temporal resolution of the ERA-Interim pressure fields, as well as a tendency of these schemes to split ECL tracks in cases with complex centers or rapid changes (Pepler and Coutts-Smith 2013). As a consequence, the interannual variability is substantially higher in these methods than the MLD.

The exception is the ULGV method, which identifies twice as many ECL days, and substantially more days associated with weather impacts, than the direct ECL identification methods. This is in large part due to the use of a 48-h running mean of maximum ULGV; when the ULGV is instead calculated using a 12-h running mean the number of ECL days per year decreases to 44.9 p.a. across the same number of events, with substantially fewer instances persisting beyond 2 days (Fig. 3).

It is also important to note the temporal resolution, with 6-hourly pressure data used for the automated ECL identification methods but only 0000 UTC data available for the MLD. This improves the ability of the ECL tracking methods to identify the start and end date of events as well as rapidly moving or developing ECLs, but may also result in multiple ECL tracks for an event identified as a single system in the MLD. These split tracks can be a consequence of complex low development in the real world, making it difficult to define a "true" correct track for an individual event that may have multiple centers or periods of decay and reintensification (e.g., Baehr et al. 1999). Such events are
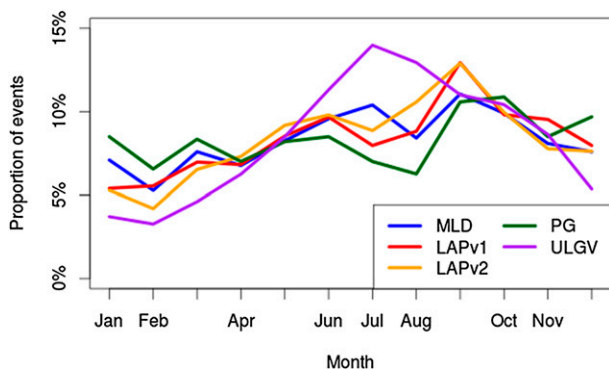
FIG. 4. Seasonal distribution of ECL events (1980–2009) for the MLD and the four automated ECL identification methods described in section 2.

often simplified in the MLD, with only the main low center retained, but can result in varying ECL tracks across different automated methodologies. Split tracks can also arise as an artifact of the low tracking procedure itself, with split tracks leading to erroneously high cyclone counts for a given intensity threshold (e.g., Mesquita et al. 2009).

When the thresholds used in this paper for the automated schemes were instead applied to 0000 UTC data only, for the best comparison with MLD resolution, the number of ECL days identified using the PG and LAP methods was halved. Therefore, the event-based approach may unfairly penalize the LAP and PG methods when compared to the ULGV. For this reason, Pepler and Coutts-Smith (2013) found that a weaker intensity threshold (and correspondingly a larger frequency of events) was needed to accurately detect the weaker ECLs in the MLD.

While the majority of approaches identify a peak in ECL frequency during the June–October period, the extent of the seasonality also varies between the different approaches (Fig. 4). The most pronounced seasonality is observed for the ULGV method, with 60% of ECLs observed between June and October and just 12% during summer (December–February), while the weakest seasonality is found using the PG method. The seasonality of the number of days with an ECL observed is similar to that for the number of distinct ECL events for each method, which suggests reduced seasonality is not a consequence of ''splitting'' of events.

Interannual variations also differ between methods, with correlations between numbers of ECL events in the MLD and the automated methods ranging between 0.52 (LAPv1) and 0.58 (ULGV). Correlations between the three surface low identification methods are strong during the cool season (May–October), with generally weaker correlations during the warm season (November–April)

TABLE 2. Pearson's correlation between annual numbers of ECL events identified by each method for (lower left) May–October and (top right) November–April; boldface font indicates statistically significant correlations at the 5% level using a Student's *t* test.

		Nov–Apr				
		MLD	LAPv1	LAPv2	PG	ULGV
May–Oct	MLD	—	**0.50**	**0.45**	**0.49**	−0.04
	LAPv1	**0.56**	—	**0.75**	**0.54**	0.08
	LAPv2	**0.50**	**0.79**	—	0.21	0.11
	PG	**0.47**	**0.91**	**0.74**	—	0.10
	ULGV	**0.54**	0.34	0.25	0.26	—

(Table 2). This is likely related to an increased frequency of marginal and weak events during the warm season, allowing for larger differences in detection between methods.

Even during the cool season, variations in the numbers of events detected by the different methods have a strong influence on the apparent relationship between cool season ECLs and the El Niño–Southern Oscillation (ENSO; Table 3). While results using the MLD, or the ULGV method, suggest little influence of ENSO on ECL frequency, the LAPv1, LAPv2, and PG methods all identify fewer ECLs during El Niño winters.

This is consistent with a large range of relationships between ECLs and ENSO reported from studies that used different time periods and identification methods (Hopkins and Holland 1997; Browning and Goodwin 2013; Pepler et al. 2014). This may reflect differences in the types of ECL identified by different methods, and affirms the need to analyze ECLs in terms of their synoptic situation (e.g., Browning and Goodwin 2013) when analyzing relationships with climate drivers. Importantly, despite varying trends in ECLs identified over different periods (Hopkins and Holland 1997; Speer et al. 2009) and strong future declines predicted (Dowdy et al. 2014, 2013c; Ji et al. 2014, manuscript submitted to *Climate Dyn.*), no methods in this paper identified any statistically significant trends in ECLs between 1980 and

TABLE 3. Pearson's correlation of May–October ECL events and the concurrent Southern Oscillation index, an indicator of ENSO; boldface font indicates statistically significant correlations at the 5% level using a Student's *t* test. The table also shows the average ECL frequencies by ENSO state (from http://www.bom.gov.au/climate/enso/enlist).

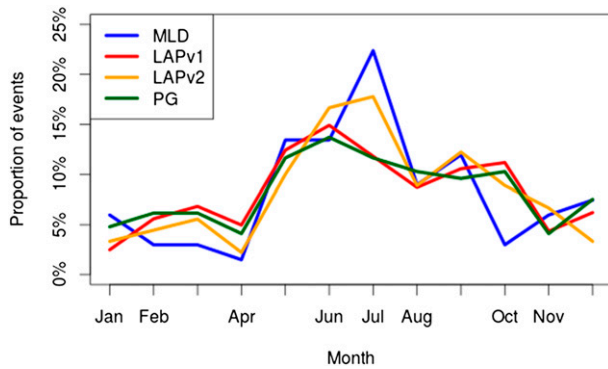| May–Oct	MLD	LAPv1	LAPv2	PG	ULGV
Correlation (all events)	0.17	**0.53**	**0.72**	**0.51**	0.13
El Niño	12	10.8	9.8	9.1	14.5
Neutral	13.7	14.7	14.4	12.2	16.2
La Niña	11.8	14.8	15.0	13.3	14.0

FIG. 5. Seasonal distribution (1980–2009) of ECL ''bomb'' events for the MLD and the three ECL identification methods (section 2), which have pressure data for individual ECL events.

2009 using a linear least squares regression, with decadal mean frequencies varying by less than 10%.

Of particular interest is the detection of so-called explosive cyclones, or bombs, which formed 11% of the MLD but accounted for 22% of ECLs associated with high waves and 33% of those with strong winds. Using the 6-h normalized deepening rate described in section 2, the automated methods identified between 14% (LAPv2) and 23% (PG) of events per year as bombs. In contrast to Fig. 3, all methods show a clear winter dominance of explosive events (Fig. 5), with 35%–45% of bombs occurring during winter (June–August) and approximately 70% of bombs occurring between May and October. This is consistent with studies such as Sanders and Gyakum (1980), which identified approximately 75% of 12-h bombs in the Northern Hemisphere between November and March, while Allen et al. (2010) found approximately 40% of 24-h bombs in the Southern Hemisphere were during June–August.

5. Event matching and detection

A key issue is to determine to what extent do the various automated ECL identification methods identify the same events, and in what ways they differ. This is first assessed using the MLD as a reference point, as it is expected to identify the majority of ECLs with significant impacts.

As discussed in section 2, we consider an ECL a hit if an automated method has an ECL identified within ±1 day of the MLD event, and a false alarm if no MLD ECL exists within ±1 day of the automated ECL. Hit rates varied between 67.5% (ULGV) and 57.9% (PG) (Fig. 6), with 42% of events detected by all four methods. False alarm rates were also highest for the ULGV method (39%), decreasing to 31% for the PG method, 24% for LAPv2 and 22% for LAPv1. Based on these metrics, the LAPv2 method could be considered the ''best'' method, with the highest CSI (0.55). However, it is important to understand the performance of each detection method across a wide range of ECLs.

The MLD can be divided into six types of events, which can be broadly categorized as those that develop from the midlatitude westerlies and those that develop in prevailing easterly onshore flow. While the hit rates for easterly events are relatively consistent across
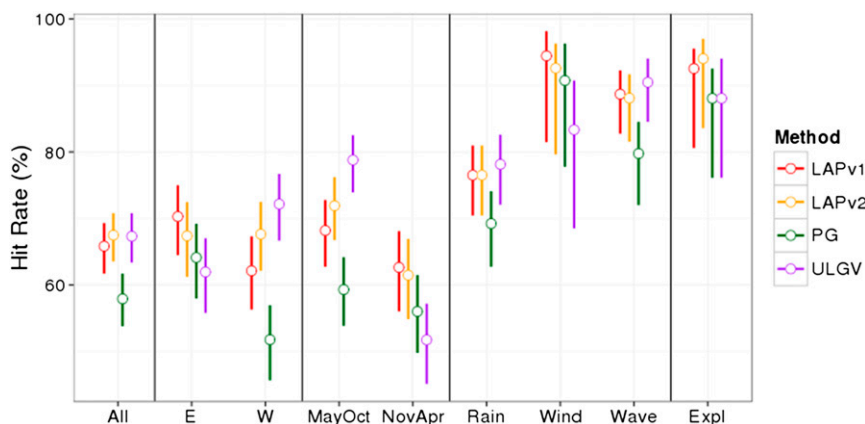

FIG. 6. Hit rates (within 1 day) for the four ECL identification methods (section 2) when detecting ECL events in the MLD, with bars indicating the 95% confidence interval from a using the bias-corrected accelerated bootstrap test (10 000 samples). Hit rates for subcategories of ECL are also indicated, including easterly (E) and westerly (W) events; those in the cool (May–October) and warm (November–April) seasons; those associated with an east coast rainfall cluster, wind gusts >90 km h^{-1}, or significant wave heights >4 m; and explosive events.

methods, detection of westerly events is substantially higher for the ULGV method, and lower for the PG method (Fig. 6). This is predominantly due to wave on a front (WF) events, which occur when a low center with associated fronts develops from the midlatitude westerlies (Speer et al. 2009, their Fig. 3d), and form 35% of the MLD database. Hit rates for these events range from 53% (PG) to 79% (ULGV), strongly influencing overall hit rates; when they are excluded from the analysis, hit rates are 60% for the PG and ULGV methods, and 66% for the two LAP methods.

It is unclear why WF events are detected with such varying skill between methods, particularly as these events tend to have stronger central pressures recorded in the MLD database, with an average central pressure 3 hPa lower than that for easterly events. One possible cause is the presence of strong frontal waves, which can have very low pressures without a true low pressure center. These are explicitly considered as part of the ULGV method, which does not require a surface low; although they are not included in the MLD, the use of human pattern recognition may make a small low center more likely to be identified. They may also be better detected through use of the Laplacian than pressure gradients, particularly as the LAP method includes the option for open systems. However, only 5% of ECLs in the LAPv2 database would be removed if open systems were excluded, with WF lows no more likely than any other ECL type to be detected as open systems.

While WF events are also the most southerly, with a mean latitude of 36.8°S compared to 34.1°S for all other events, hit rates are at least 10% higher for WF events south of 35°S than those farther north for methods other than ULGV, suggesting this is not the reason. Furthermore, WF events detected by the LAPv2 method (which provides additional low statistics) are, on average, larger and slower moving than other systems, which would be expected to increase detection rates for all methods. Further research will be needed into the reasons for the variable skill for these WF events.

Hit rates are generally higher in the cool season, particularly for those methods with improved detection of westerly events, consistent with results observed in Dowdy et al. (2013a) and Pepler and Coutts-Smith (2013). Surprisingly, however, this pattern is not related to the relative proportion of westerly events, which form 61% of cool season ECLs but only 38% of warm season ECLs. During the warm season the difference in skill between westerly and easterly events is less than 5% for all methods, while the only method with a substantial increase in the cool season hit rate for westerly events is ULGV (+29%). Instead, the major influence is

varying skill in *easterly* events—all methods have hit rates of at least 75% for easterly events during the cool season, between 15% (LAPv1) and 27% (ULGV) higher than the hit rate for all events during the cool season.

Pepler and Coutts-Smith (2013) attributed the lower warm season hit rates to a tendency for smaller and weaker ECLs during the summer months. This appears to be the case for LAPv2, which is the only method to output the radius of the detected low, with average radiuses 0.5° smaller in the warm season and 47% of events detected with radiuses below 5° (22% in the cool season). The minimum radius of any low using this method was 3.0°, so it is possible that yet smaller lows have been missed. The choice of radius for low identification appears to be most important during the warm season; when a low radius of 5° is used for calculating the intensity of lows, the warm season hit rates for both the LAP methods decrease by 7%–8%, with little change in cool season ECL detection.

Importantly, all methods detect more than 80% of ECLs associated with explosive development large waves, or strong winds. While hit rates appear slightly higher for the LAP methods, differences are not statistically significant using a binomial test. All methods are also more likely to detect events with deeper central pressures or longer durations (Fig. 7), including at least 75% of the 229 ECLs with central pressures below 1000 hPa; 81% of these events are identified by at least three of the tracking schemes. In comparison, only the ULGV method manages to detect more than 40% of the 127 events with central pressures above 1010 hPa.

Unsurprisingly, of the 92 events in the MLD that were not detected by any automated method, only 9 had minimum pressures below 1000 hPa, and only 9 persisted for more than two days. These results are expected, as Pepler and Coutts-Smith (2013) identified numerous weak events in the MLD where the identification of a low was relatively arbitrary, and the use of intensity-based thresholds in restricting the ECL datasets is most likely to decrease detection of such events.

An investigation of these 92 "missed" events found they mostly occurred during the warm season, with 27% of ECLs in the MLD missed by all automated methods during summer (December–February), but only 8% of events missed during the main ECL season June–August. Only one event with strong winds or waves was missed by all four automated methods, although 24% of missed ECLs were associated with rain impacts. This reflects the inclusion of several events with weak or small lows embedded in a coastal trough or onshore flow, which can cause substantial rain in coastal Australia even in the absence of an ECL.
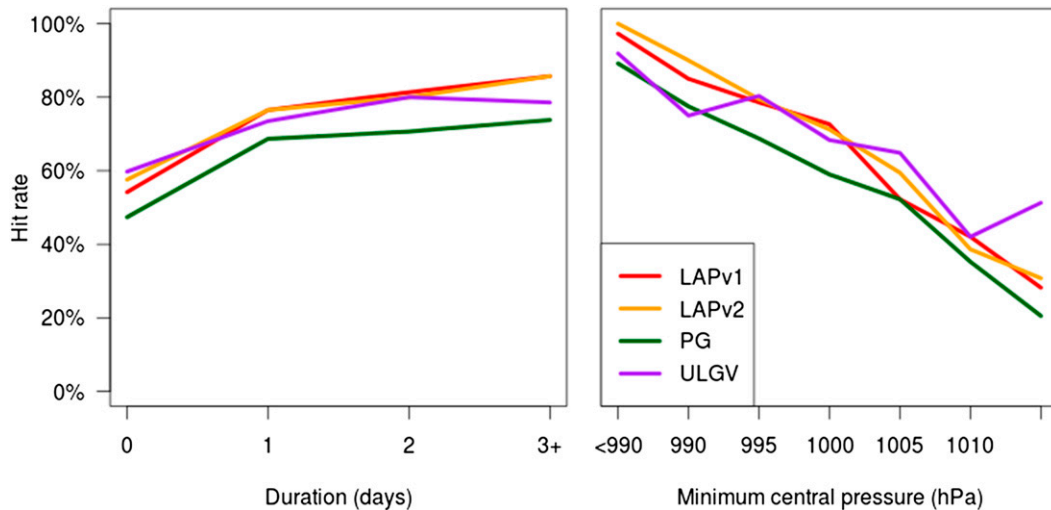
FIG. 7. Hit rates (within 1 day) for the four ECL identification methods (section 2) when detecting ECL events in the MLD as a function of (left) duration and (right) central pressure.

In addition to their detection of ECLs in the MLD, it is also useful to understand the similarities between the four automated methods. One way to test this is in terms of the ECL days, with the CSI between two automated methods reflecting the proportion of cases where both identify the same ECL day (Table 4). Using this method, at least 50% of ECL days are common between the LAPv1, LAPv2, and PG methods. The similarities between these three methods are particularly evident for the more intense ECLs—of the 517 days with curvatures above $1.5\,hPa$ $(°lat)^{-2}$ using LAPv1, 92% also have ECLs identified using both the LAPv2 and PG methods, as well as 96% of days with curvature greater than $2\,hPa$ $(°lat)^{-2}$.

The ULGV method uses a very different approach, and understandably has a weaker relationship with lows identified by the other tracking schemes. This is partly related to the larger number of ECL-favorable days identified, and consequently high ''false alarm'' rates. Intensity of the ULGV is also a weaker indicator of the presence of an ECL, as only 52% of the 150 largest ULGV days have a corresponding ECL in the MLD (74% within ±1 day) and only 73% have an ECL within ±1 day using any of the other automated methods. The ULGV method, while successfully identifying the majority of strong wave events (Dowdy et al. 2014), is evidently identifying different systems to those in the other methods. This is to be expected, as strong upper-level lows may have strong weather impacts without a corresponding surface low.

For all cases but the ULGV method, it is also possible to identify the location of an individual ECL. Corresponding to the large CSI values, 85% of lows identified

with the PG method have a corresponding low at the same time and within 1.5° (one grid point) using LAPv1, as do 75% of lows identified using LAPv2, with lower agreements between LAPv2 and PG. Notably, where there is a low in any two automated tracking methods at the same time, it is within 1.5° (one grid point) in more than 88% of cases. This is reflected in very similar tracks for major ECL events (Fig. 8), with the location of the low almost identical between PG and LAPv1 and differences on the order of $\pm1°$ for LAPv2. This may be associated with the use of a polar stereographic grid, but has not been tested. These results show that, while the individual lows identified may differ between ECL tracking methods, where an ECL occurs it is likely to be assigned the same location and movement for any automated method.

6. Conclusions

This study has assessed the ECL identification methods used in three recent papers (Browning and Goodwin 2013; Dowdy et al. 2013a; Pepler and Coutts-Smith 2013), as well as a more recent version of the University of Melbourne tracking scheme (Simmonds et al. 1999;

TABLE 4. CSI table, showing the strength of the relationships between ECL days identified using the four automated ECL detection methods (section 2).

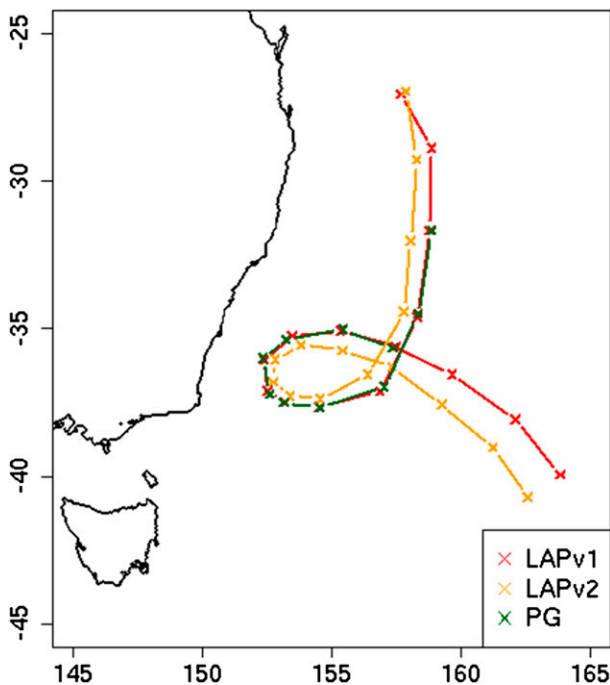|	LAPv2	PG	ULGV
LAPv1	0.67	0.65	0.24
LAPv2		0.52	0.25
PG			0.20

FIG. 8. Tracks for a low that crossed the ECL domain (Fig. 1) on 28 Jun 2007 for the three ECL identification methods (section 2), which track individual ECL events.

Lim and Simmonds 2007). These have been compared with the Speer et al. (2009) manually identified MLD to provide a useful ground truth, although the MLD is not without flaws.

All automated low tracking methods require a certain subjectivity in determining threshold criteria, so for the purposes of this study thresholds have been chosen to match the frequency of ECLs in the MLD, at 22 events p.a. Using these criteria, all four automated ECL methods successfully identify 58%–67% of ECLs in the MLD, with false alarm rates ranging between 22% (LAPv1) and 39% (ULGV). Importantly, all automated ECL identification methods identify close to 90% of ECLs in the MLD that were associated with severe waves or explosive development, and at least 75% of ECLs with central pressures below 1000 hPa. This implies that results for these more extreme ECLs will be consistent regardless of detection methods.

However, detection of weaker and midrange ECLs varies between methods. The ULGV and LAPv2 methods have improved detection of ECLs that develop from fronts or waves in the westerly flow, with improved ECL detection during the winter period. In comparison, the PG method has reduced seasonal variability and shows some improvement in detection of summer ECLs, although with correspondingly higher false alarm rates during this season.

The ULGV method identifies broader periods that favor ECL development, rather than identifying surface lows. This may have advantages in terms of the detection of significant impacts in the absence of a surface low (e.g., Dowdy et al. 2014), but precludes its use for studies of the locations, movement, or development of individual events, and increases the likelihood of ''ECLs'' being indicated in the absence of a surface low.

When an ECL is detected by all three tracking approaches, its development and movement is highly consistent across methods, with lows located within one grid point in more than 88% of instances where a low is identified by multiple methods. This is important for studies that focus on the development of individual systems, where the choice of tracking approach is unlikely to have major impacts.

One surprising result is that, for the same numbers of ECL events, the observed relationship between the frequency of ECLs and ENSO can be quite different between methodologies. While Pepler et al. (2014) found little relationship between ENSO and ECL-associated rainfall using the MLD, a statistically significant relationship with ENSO is observed for both the LAP and PG methods, with a notable decline in ECLs during El Niño years. This demonstrates that the relationship between ECLs and climate drivers is very sensitive to the definition used, helping to explain the variety of relationships observed in the literature (e.g., Hopkins and Holland 1997; Browning and Goodwin 2013). This will necessitate further research into the best way of assigning ECL ''types'' to tracking schemes to better categorize different relationships, potentially using the backtracking approach of Browning and Goodwin (2013) or the cyclone phase-space model of Hart (2003).

Future research will focus on the LAPv2 method, as it has the highest CSI score as well as more advanced low tracking capability. However, skill is lower for lows during the warm season, while Dowdy et al. (2013a,b,c) recommend the ULGV method for GCMs with coarse spatial resolutions. Future work will apply these low tracking algorithms to a number of global and regionally downscaled climate models, to test whether some methods are of particular use for investigating future changes in ECL occurrence or characteristics, as well as the use of climate models for testing the influences on ECL development. Future work will also seek to understand the detailed development of low pressure systems, including their warm/cold structure, to better understand the causes for varying skill with those ECLs that develop in the westerlies with associated frontal systems.

REFERENCES

Abbs, D., and Coauthors, 2006: Projections of extreme rainfall and cyclones: Final report to the Australian Greenhouse Office. CSIRO Marine and Atmospheric Research, Aspendale, Victoria, Australia, 97 pp. [Available online at https://publications.csiro.au/rpr/pub?list=SEA&pid=procite:9f7fb6b5-5433-4685-ac47-f6145c2041e2.]

Allen, J. T., A. B. Pezza, and M. T. Black, 2010: Explosive cyclogenesis: A global climatology comparing multiple reanalyses. *J. Climate,* **23,** 6468–6484, doi:10.1175/2010JCLI3437.1.

Alpert, P., B. U. Neeman, and Y. Shay-El, 1990: Climatological analysis of Mediterranean cyclones using ECMWF data. *Tellus,* **42A,** 65–77, doi:10.1034/j.1600-0870.1990.00007.x.

Baehr, C., B. Pouponneau, F. Ayrault, and A. Joly, 1999: Dynamical characterization of the FASTEX cyclogenesis cases. *Quart. J. Roy. Meteor. Soc.,* **125,** 3469–3494, doi:10.1002/qj.49712556117.

Browning, S. A., and I. D. Goodwin, 2013: Large-scale influences on the evolution of winter subtropical maritime cyclones affecting Australia's east coast. *Mon. Wea. Rev.,* **141,** 2416–2431, doi:10.1175/MWR-D-12-00312.1.

Callaghan, J., and P. Helman, 2008: Severe storms on the east coast of Australia, 1770-2008. Griffith Centre for Coastal Management, Griffith University, Gold Coast, Queensland, Australia, 240 pp. [Available online at http://www.goldcoast.qld.gov.au/documents/bf/storms-east-coast-1770-2008.pdf.]

Chambers, C. R. S., G. B. Brassington, I. Simmonds, and K. Walsh, 2014: Precipitation changes due to the introduction of eddy-resolved sea surface temperatures into simulations of the ''Pasha Bulker'' Australian east coast low of June 2007. *Meteor. Atmos. Phys.,* **125,** 1–15, doi:10.1007/s00703-014-0318-4.

Dee, D. P., and Coauthors, 2011: The ERA-Interim reanalysis: Configuration and performance of the data assimilation system. *Quart. J. Roy. Meteor. Soc.,* **137,** 553–597, doi:10.1002/qj.828.

Dowdy, A. J., G. A. Mills, and B. Timbal, 2011: Large-scale indicators of Australian east coast lows and associated extreme weather events. Centre for Australian Weather and Climate Research, Tech. Rep. 37, 102 pp. [Available online at http://cawcr.gov.au/publications/technicalreports/CTR_037.pdf.]

——, ——, and ——, 2013a: Large-scale diagnostics of extratropical cyclogenesis in eastern Australia. *Int. J. Climatol.,* **33,** 2318–2327, doi:10.1002/joc.3599.

——, ——, ——, M. Griffiths, and Y. Wang, 2013b: Understanding rainfall projections in relation to extratropical cyclones in eastern Australia. *Aust. Meteor. Ocean J.,* **63,** 355–364.

——, ——, ——, and Y. Wang, 2013c: Changes in the risk of extratropical cyclones in eastern Australia. *J. Climate,* **26,** 1403–1417, doi:10.1175/JCLI-D-12-00192.1.

——, ——, ——, and ——, 2014: Fewer large waves projected for eastern Australia due to decreasing storminess. *Nat. Climate Change,* **4,** 283–286, doi:10.1038/nclimate2142.

Grieger, J., G. C. Leckebusch, M. G. Donat, M. Schuster, and U. Ulbrich, 2014: Southern Hemisphere winter cyclone activity under recent and future climate conditions in multi-model AOGCM simulations. *Int. J. Climatol.,* **34,** 3400–3416, doi:10.1002/joc.3917.

Hart, R. E., 2003: A cyclone phase space derived from thermal wind and thermal asymmetry. *Mon. Wea. Rev.,* **131,** 585–616, doi:10.1175/1520-0493(2003)131<0585:ACPSDF>2.0.CO;2.

Hewson, T. D., 2009: Diminutive frontal waves—A link between fronts and cyclones. *J. Atmos. Sci.,* **66,** 116–132, doi:10.1175/2008JAS2719.1.

Hope, P., and Coauthors, 2014: A comparison of automated methods of front recognition for climate studies: A case study in southwest Western Australia. *Mon. Wea. Rev.,* **142,** 343–363, doi:10.1175/MWR-D-12-00252.1.

Hopkins, L. C., and G. J. Holland, 1997: Australian heavy-rain days and associated east coast cyclones: 1958–92. *J. Climate,* **10,** 621–635, doi:10.1175/1520-0442(1997)010<0621:AHRDAA>2.0.CO;2.

Hoskins, B. J., and K. I. Hodges, 2005: A new perspective on Southern Hemisphere storm tracks. *J. Climate,* **18,** 4108–4129, doi:10.1175/JCLI3570.1.

Jones, D. A., and I. Simmonds, 1993: A climatology of Southern Hemisphere extratropical cyclones. *Climate Dyn.,* **9,** 131–145, doi:10.1007/BF00209750.

——, W. Wang, and R. Fawcett, 2009: High-quality spatial climate data-sets for Australia. *Aust. Meteor. Ocean J.,* **58,** 233–248.

Kalnay, E., and Coauthors, 1996: The NCEP/NCAR 40-Year Reanalysis Project. *Bull. Amer. Meteor. Soc.,* **77,** 437–471, doi:10.1175/1520-0477(1996)077<0437:TNYRP>2.0.CO;2.

King, A. D., L. V. Alexander, and M. G. Donat, 2013: The efficacy of using gridded data to examine extreme rainfall characteristics: A case study for Australia. *Int. J. Climatol.,* **33,** 2376–2387, doi:10.1002/joc.3588.

König, W., R. Sausen, and F. Sielmann, 1993: Objective identification of cyclones in GCM simulations. *J. Climate,* **6,** 2217–2231, doi:10.1175/1520-0442(1993)006<2217:OIOCIG>2.0.CO;2.

Kouroutzoglou, J., H. A. Flocas, K. Keay, I. Simmonds, and M. Hatzaki, 2011: Climatological aspects of explosive cyclones in the Mediterranean. *Int. J. Climatol.,* **31,** 1785–1802, doi:10.1002/joc.2203.

Lim, E.-P., and I. Simmonds, 2002: Explosive cyclone development in the Southern Hemisphere and a comparison with Northern Hemisphere events. *Mon. Wea. Rev.,* **130,** 2188–2209, doi:10.1175/1520-0493(2002)130<2188:ECDITS>2.0.CO;2.

——, and ——, 2007: Southern Hemisphere winter extratropical cyclone characteristics and vertical organization observed with the ERA-40 data in 1979–2001. *J. Climate,* **20,** 2675–2690, doi:10.1175/JCLI4135.1.

Mesquita, M. S., D. E. Atkinson, I. Simmonds, K. Keay, and J. Gottschalck, 2009: New perspectives on the synoptic

development of the severe October 1992 Nome storm. *Geophys. Res. Lett.,* **36,** L13808, doi:10.1029/2009GL038824.

Mills, G. A., R. Webb, N. E. Davidson, J. Kepert, A. Seed, and D. Abbs, 2010: The Pasha Bulker east coast low of 8 June 2007. CAWCR Tech. Rep. 023, 72 pp. [Available online at http://cawcr.gov.au/publications/technicalreports/CTR_023.pdf.]

Murray, R. J., and I. Simmonds, 1991: A numerical scheme for tracking cyclone centres from digital data. Part I: Development and operation of the scheme. *Aust. Meteor. Mag.,* **39,** 155–166.

Neu, U., and Coauthors, 2013: IMILAST: A community effort to intercompare extratropical cyclone detection and tracking algorithms. *Bull. Amer. Meteor. Soc.,* **94,** 529–547, doi:10.1175/BAMS-D-11-00154.1.

Pepler, A. S., and C. S. Rakich, 2010: Extreme inflow events and synoptic forcing in Sydney catchments. *IOP Conf. Ser. Earth Environ. Sci.,* **11,** 012010, doi:10.1088/1755-1315/11/1/012010.

——, and A. Coutts-Smith, 2013: A new, objective, database of East Coast Lows. *Aust. Meteor. Ocean J.,* **63,** 461–472.

——, ——, and B. Timbal, 2014: The role of East Coast Lows on rainfall patterns and inter-annual variability across the East Coast of Australia. *Int. J. Climatol.,* **34,** 1011–1021, doi:10.1002/joc.3741.

Pezza, A. B., and T. Ambrizzi, 2003: Variability of Southern Hemisphere cyclone and anticyclone behavior: Further analysis. *J. Climate,* **16,** 1075–1083, doi:10.1175/1520-0442(2003)016<1075: VOSHCA>2.0.CO;2.

Pinto, J. G., T. Spangehl, U. Ulbrich, and P. Speth, 2005: Sensitivities of a cyclone detection and tracking algorithm: Individual tracks and climatology. *Meteor. Z.,* **14,** 823–838, doi:10.1127/0941-2948/2005/0068.

Qi, L., L. M. Leslie, and M. S. Speer, 2006: Climatology of cyclones over the southwest Pacific: 1992–2001. *Meteor. Atmos. Phys.,* **91,** 201–209, doi:10.1007/s00703-005-0149-4.

Sanders, F., and J. R. Gyakum, 1980: Synoptic-dynamic climatology of the ''bomb.'' *Mon. Wea. Rev.,* **108,** 1589–1606, doi:10.1175/1520-0493(1980)108<1589:SDCOT>2.0.CO;2.

Simmonds, I., R. J. Murray, and R. M. Leighton, 1999: A refinement of cyclone tracking methods with data from FROST. *Aust. Meteor. Mag.,* Special Edition, 35–49. [Available online at http://www.bom.gov.au/amoj/docs/1999/simmonds.pdf.]

——, C. Burke, and K. Keay, 2008: Arctic climate change as manifest in cyclone behavior. *J. Climate,* **21,** 5777–5796, doi:10.1175/2008JCLI2366.1.

Sinclair, M. R., 1994: An objective cyclone climatology for the Southern Hemisphere. *Mon. Wea. Rev.,* **122,** 2239–2256, doi:10.1175/1520-0493(1994)122<2239:AOCCFT>2.0.CO;2.

Speer, M. S., P. Wiles, and A. Pepler, 2009: Low pressure systems off the New South Wales coast and associated hazardous weather: Establishment of a database. *Aust. Meteor. Ocean J.,* **58,** 29–39.

Uotila, P., A. B. Pezza, J. J. Cassano, K. Keay, and A. H. Lynch, 2009: A comparison of low pressure system statistics derived from a high-resolution NWP output and three reanalysis products over the Southern Ocean. *J. Geophys. Res.,* **114,** D17105, doi:10.1029/2008JD011583.

——, T. Vihma, A. B. Pezza, I. Simmonds, K. Keay, and A. H. Lynch, 2011: Relationships between Antarctic cyclones and surface conditions as derived from high-resolution numerical weather prediction data. *J. Geophys. Res.,* **116,** D07109, doi:10.1029/2010JD015358.

Wernli, H., and C. Schwierz, 2006: Surface cyclones in the ERA-40 dataset (1958–2001). Part I: Novel identification method and global climatology. *J. Atmos. Sci.,* **63,** 2486–2507, doi:10.1175/JAS3766.1.